

Smart mounts

A novel active vibration isolation approach using stiff supports (called hard mounts) is discussed. The objective of this vibration isolation system is to combine high support stiffness with excellent isolation of floor vibrations. The support stiffness is realized by mechanical design and the floor vibration isolation performance is realized by means of feedback and adaptive feedforward control. This constitutes a novel approach to vibration isolation, which is not offered by manufacturers of vibration isolation systems.

• ***Tjeerd van der Poel, Johannes van Dijk, Ben Jonker and Herman Soemers*** •

Vibrations due to environmental disturbances can cause a loss of accuracy in high-precision equipment. This is illustrated schematically in Figure 1. In many cases, floor vibrations are the dominant mechanical disturbance source. To reduce the vibration levels due to floor motion, the equipment is commonly mounted on vibration isolation systems with relatively low support stiffness. However, the low stiffness of such soft suspension systems may introduce difficulties in the response to direct disturbances (e.g. reaction forces due to stage motion or cable-

transmitted forces) and with the levelling of the equipment. The high support stiffness in hard mounts circumvents these difficulties.

In a recent Mikroniek article [2], an overview of the basics and common concepts in (active) vibration isolation systems was presented. The active hard mount vibration isolation approach discussed here is an extension of the “piezo solution” that was briefly touched upon in that article. However, the key element in this approach is the

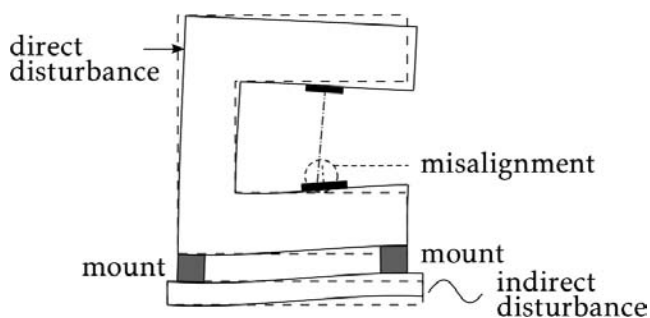


Figure 1. Illustration of deformations in a machine due to various disturbances, leading to a reduction in the machine accuracy.

Authors

Herman Soemers is part-time professor of Mechatronic Design, Ben Jonker is full professor of Machine Dynamics and Robotics, and Johannes van Dijk is assistant professor of Mechatronics. All are with the Laboratory of Mechanical Automation and Mechatronics at the University of Twente, Enschede, the Netherlands. Tjeerd van der Poel has obtained his Ph.D. degree [1] on the topic of active hard mount vibration isolation in the same research group.

j.vandijk@utwente.nl
www.wa.ctw.utwente.nl

high suspension stiffness, which need not necessarily be realized by piezoelectric actuators.

Design guidelines

Figure 2 shows a mass-spring-damper model of a suspended machine, which captures the basic features of a vibration isolation problem. Note that this machine model contains a structural resonance mode, because such structural modes typically occur within the frequency range of interest. In many cases, the internal deformation ($\Delta x = x_2 - x_1$) determines to a large extent the machine accuracy. At frequencies up to the first structural resonance, this deformation is proportional to the acceleration level of the machine $\ddot{x}_1(t)$. Therefore, the response of the supported machine to floor vibrations and direct disturbance forces is usually considered. This response is described in the frequency domain by the transmissibility function $T(j\omega)$ and the dynamic compliance $C_1(j\omega)$:

$$T(j\omega) = \frac{x_1(j\omega)}{x_0(j\omega)} = \frac{\text{machine motion}}{\text{floor vibration}} \quad (\text{Equation 1})$$

$$C_1(j\omega) = \frac{x_1(j\omega)}{F_{d1}(j\omega)} = \frac{\text{machine motion}}{\text{direct disturbance force}} \quad (\text{Equation 2})$$

The support stiffness offers a distinct trade-off in the design of a vibration isolation system. This trade-off is illustrated in Figure 3 in terms of the transmissibility and

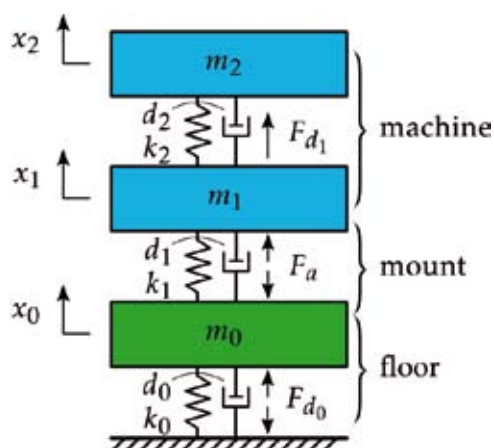


Figure 2. Basic model of the vibration isolation problem.

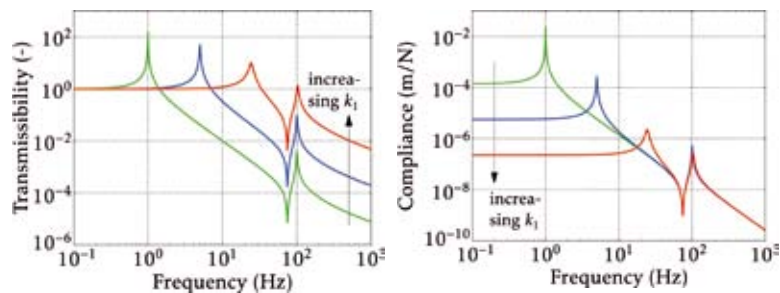


Figure 3. Design trade-off for the support stiffness k_i : effect on the transmissibility $T(j\omega)$ and the compliance $C_1(j\omega)$.

compliance. In words, low stiffness offers good isolation of floor vibrations, but increases the sensitivity to direct disturbance forces. For hard mounts, the opposite is true.

Due to the relatively high support stiffness of hard mounts, an exact constraint design of the support system is necessary. This means that all the “rigid body” degrees of freedom of the machine (i.e. three translations and three rotations) are constrained exactly once. Otherwise, difficulties with thermal loads and manufacturing and assembly tolerances are likely to occur [3].

Moreover, deviating from the exact constraint design can have a significant effect on the realizable vibration isolation performance. The so-called parasitic stiffness in the mount offers additional transfer paths for vibration energy, which are extremely difficult to suppress using active control. Figure 4 shows the effects of parasitic stiffness in the mounts on the transmissibility of the active hard mount system; see [1] for details. As a rule of thumb, the parasitic stiffnesses must be at least 100 times lower than the principal stiffness.

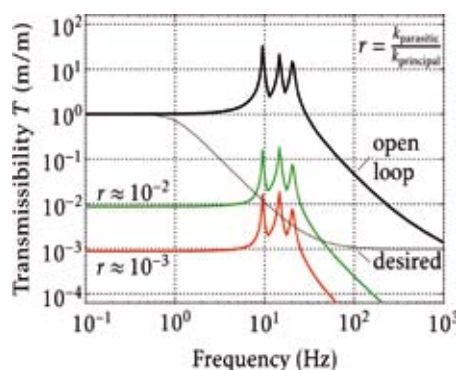


Figure 4. Effect of parasitic stiffness on the (best case) floor vibration transmissibility.

Active control strategy

From Figure 3, it is clear that the transmissibility of a hard mounted system has to be improved significantly to achieve the same vibration isolation performance as a soft suspension system. For this purpose an active control system is used that combines feedback control of the

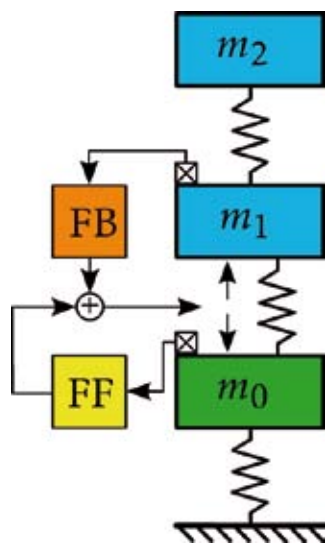


Figure 5. Combined feedback (FB) and feedforward (FF) control using absolute motion sensors (geophones or accelerometers).

machine motion with feedforward compensation of the measured floor vibrations; see Figure 5. Note that all active components (sensors, actuators) are placed in the

mount, resulting in a modular system. The feedback control aims at adding active damping to the suspension and relevant structural resonances in the system. The transmission of floor vibrations is then reduced further by the feedforward compensation. This feedforward controller generates anti-forces based on the measured floor vibration, attempting to cancel the machine vibrations induced by the floor vibrations.

Active damping

The feedback control strategy is based on Direct Velocity Feedback (DVF) [4], which uses collocated actuator/sensor pairs to effectively add viscous dampers at the actuation points in the system. Due to the collocation, the decentralized feedback loops are robustly stable. The theoretical maximum damping ratio for a carefully tuned DVF controller is given by

$$\zeta_{\max} = \begin{cases} \frac{1}{2} \left(\frac{\omega_r}{\omega_a} - 1 \right) & \text{if } \omega_a < \omega_r; \\ \frac{1}{2} \left(\frac{\omega_a}{\omega_r} - 1 \right) & \text{if } \omega_a > \omega_r, \end{cases} \quad (\text{Equation 3})$$

where ω_r is the natural frequency of the structural resonance mode to which the DVF controller is tuned and ω_a is the anti-resonance frequency closest to ω_r . As a result, the spacing (in the frequency domain) of the structural resonance and anti-resonance frequencies is of key importance for the achievable damping.

In view of this result, it can be shown that either geophones or accelerometers are the preferred choice of sensors (compared to force sensors and displacement sensors). Throughout this research project, accelerometers have been used. These sensors provide the largest spacing of ω_a and ω_r . Moreover, with these sensors it is possible to achieve skyhook damping of the suspension modes of the

supported machine. This means that damping can be added while retaining the -40 dB/decade roll-off in the transmissibility function. When using relative damping, the roll-off would reduce to -20 dB/decade, leading to an increase in transmissibility at high frequencies.

Feedforward compensation of floor vibrations

A block diagram of the feedforward control system is shown in Figure 6. The components in the block diagram have the following interpretation:

- $P(z)$: primary path; describes the system dynamics relating the disturbance source $d(k)$ and the machine acceleration $\ddot{x}_1(k)$. (or an equivalent sensor signal)
- $S(z)$: secondary path; describes the system dynamics relating the control force $F_a(k)$ and the machine acceleration $\ddot{x}_1(k)$.
- $T(z)$: tertiary path; describes the system dynamics relating the disturbance source $d(k)$ and the floor acceleration $\ddot{x}_0(k)$. (or an equivalent sensor signal)
- $W(z)$: feedforward controller
- $d(k)$: disturbance source, assumed to be a white noise signal; the colouring of the floor vibration spectrum is achieved by including a spectral factor into $T(z)$ and $P(z)$.
- $r(k)$: reference signal for the feedforward controller; this signal represents the floor acceleration $\ddot{x}_0(k)$ due to the disturbance source $d(k)$.

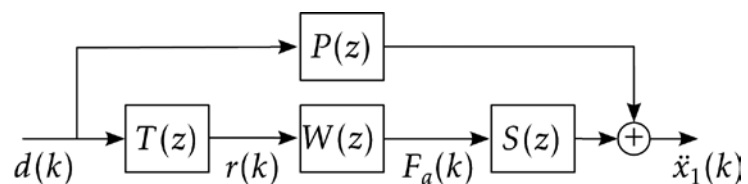


Figure 6. Block diagram of the feedforward control system.

The transfer functions $P(z)$, $S(z)$ and $T(z)$ represent the closed-loop system dynamics, i.e. including the feedback control. Moreover, the reference signal $r(k)$ is obtained from the measured floor acceleration $\ddot{x}_0(k)$ by compensating for the effect of the control force $F_a(k)$ on the floor acceleration, using internal model compensation (IMC). The IMC is required to prevent instability of the feedforward compensation. Furthermore, the signals and transfer functions are presented in the discrete domain, because the feedforward controller is implemented digitally.

Theoretically, the optimal feedforward controller $W_o(z)$ is given by:

$$W_o(z) = -S^{-1}(z)P(z)T^{-1}(z) \quad (\text{Equation 4})$$

However, the inverses indicated in Equation 4 may result in an unstable and/or acausal optimal controller, which can not be implemented in practice. Moreover, the system dynamics $P(z)$ and $T(z)$ are difficult to obtain in practice. Therefore, an adaptive algorithm is used to find an approximation of the optimal feedforward controller. Moreover, the adaptive nature of the controller offers (to some extent) tracking capabilities for time-varying disturbances.

Commonly, the feedforward control force $F_a(k)$ is computed as a weighted summation of delayed samples of the reference signal $r(k)$, see Equation 5.

$$F_a(k) = \sum_{l=1}^L w_l(k)r(k-l+1) \quad (\text{Equation 5})$$

This is called a Finite Impulse Response (FIR) parametrization because the weight vector $w(k)$ contains the impulse response coefficients of the controller and its length is limited to the user-defined number L . The controller weights are updated using the filtered-reference least mean squares (FxLMS) algorithm [5], resulting in a convex adaptation (i.e. a unique global minimum exists). Several extensions to the standard FxLMS algorithm have been implemented to further improve the convergence rate as well as the robustness of the adaptation; see [1] for details.

A significant drawback of the FIR parametrization of the feedforward controller is the large number of coefficients that is required to accurately describe systems with long impulse responses (i.e. systems with poorly damped resonances). Unfortunately, this is typically the case in precision equipment. As a result, the achievable performance can, in practice, be limited by the real-time computational capabilities of the digital controller, especially for multi-channel vibration isolation systems.

As an alternative, an infinite impulse response (IIR) parametrization with fixed poles has been considered, see Figure 7. Its basic structure is a cascaded connection of second-order sections (SOS) and first-order sections (FOS).

Each SOS and FOS is an all-pass state-space system, which ensures that the signal power of the reference signal is transferred to all sections. The actuator force $F_a(k)$ is now formed by the weighted summation of the states of the second- and first-order sections, combined with a direct feedthrough term w_0 . This summation can be written in a similar form as Equation 5, albeit with a different reference signal. Consequently, the same adaptive algorithms can be used to update the IIR filter coefficients, and the adaptation still has a unique global minimum.

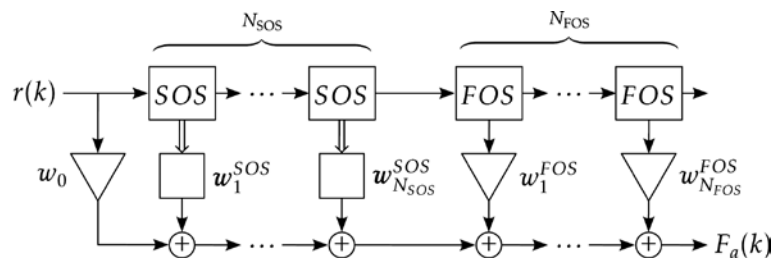


Figure 7. IIR filter parametrization: cascaded connection of N_{SOS} second-order and N_{FOS} first-order filter sections with user-selectable fixed poles. Each section is implemented as a state-space system, whose states are used to compute $F_a(k)$.

The IIR pole locations are not updated, thereby preventing the stability and convergence problems of fully adaptive IIR filters. The user should closely match all the SOS/FOS poles to the pole locations of the optimal controller. In practice, these pole locations can be chosen based on model studies, system identification and/or experimental tuning. When these pole locations are chosen correctly, a significant reduction in filter parameters (and computational complexity) can be achieved without notable degradation in performance.

As an illustrative example, assume that the optimal controller is given by the discrete transfer function

$$W_o(z) = \frac{1}{z^2 - 1.896z + 0.9937} \quad (\text{Equation 6})$$

which is a discrete, second-order, low-pass filter with poles at $0.9481 \pm 0.3080i$. These poles have a 1% damping ratio and a resonance frequency at $0.05 f_s$, where f_s is the sample frequency.

When the IIR parametrization is taken to consist of one second-order section with the exact poles of $W_o(z)$, only

two controller coefficients are required. Moreover, the IIR filter is then capable of exactly describing the optimal controller. On the other hand, the 1% settling time of this filter is 1,466 samples, i.e. it requires 1,466 samples to accurately describe the optimal controller with a FIR parametrization. Moreover, this FIR description is still only an approximation of the optimal controller.

Experimental results

The feedback and adaptive feedforward control strategies have been tested on an experimental setup, which is shown in Figure 8. The setup has only one dominant direction of motion as it is designed to mimic the basic model of Figure 2. A voice coil actuator is used as the control actuator. The linear guidance of the coil with respect to the permanent magnet is designed such that the suspension frequency of this setup is approximately 17 Hz. Therefore, the support stiffness is almost 300 times higher compared to a 1 Hz soft suspension system.

Figure 9 shows the results of various control experiments. In open-loop operation (only passive isolation, blue line), the floor vibrations mostly excite the suspension mode at 17 Hz as well as the structural resonance mode at 80 Hz. Due to the additional damping in both modes that is realized by the feedback control (red line), the machine vibration level is reduced by a factor six to 1.5 mm/s^2 (0-1,600 Hz). When the feedforward control is turned on, the machine vibration level is reduced further to 0.5 mm/s^2 (0-1,600 Hz). There is no significant difference in vibration isolation performance between the FIR (green) and IIR (purple) parametrization. However, the IIR parametrization is six times more efficient due to the significantly smaller number of coefficients, see Table 1. This table also lists the measured internal deformation.

The dominant limiting factor in the vibration isolation performance has been found to be the noise that is injected by the accelerometers and the voice coil actuator amplifier.

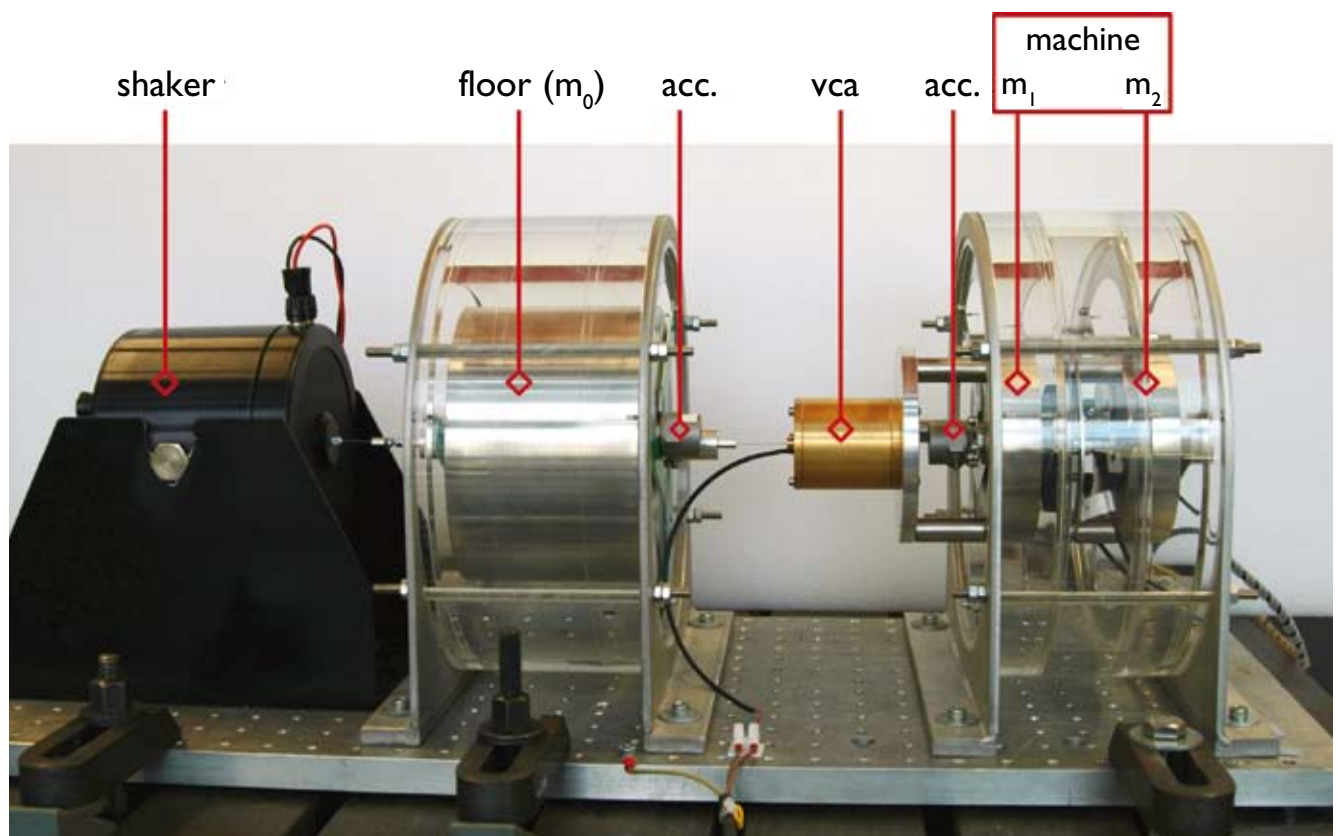


Figure 8. Experimental setup for control experiments. (acc. = accelerometer, VCA = voice coil actuator)

Table 1. Summary of control experiment results.

	Passive	Feedback	FB + FF ^c FIR	FB + FF ^c IIR	Units
\ddot{x}_0^a	7.4	6.2	6.2	6.2	mm/s ²
\ddot{x}_0^b	17	16	16	15	mm/s ²
\ddot{x}_1^a	9.4	1.4	0.25	0.14	mm/s ²
\ddot{x}_1^b	9.5	1.5	0.57	0.48	mm/s ²
Δx^a	69	10	2.9	2.7	nm
Δx^b	69	11	5.2	5.5	nm
# of FF coefficients ^c	–	–	2,000	58	–
computational time	20.4	20.9	200	31	μs

^a RMS 0-100 Hz; ^b RMS 0-1,600 Hz; ^c FB (feedback) + FF (feedforward).

Conclusions and future research

An active hard mount vibration isolation system has been discussed that allows to realize a stiff suspension system, while simultaneously offering floor vibration isolation. A combination of feedback control and (adaptive) feedforward control is used, in order to actively add damping to the suspension and structural modes and reduce the transmissibility of floor vibrations. The feasibility of this active vibration isolation concept has been demonstrated on an experimental setup with one dominant direction of motion, resulting in a 20-fold reduction in the machine acceleration level.

Future research activities will focus on implementing the control strategies on a six degrees-of-freedom hard

mounted setup and further improvement of the control performance.

References

- [1] Poel, G.W. van der (2010), “An exploration of active hard mount vibration isolation for precision equipment”, Ph.D. thesis, University of Twente, ISBN 978-90-365-3016-3.
<http://dx.doi.org/10.3990/1.9789036530163>
- [2] Bakker, B. and Seggelen, J. van (2010), “The revolutionary Hummingbird technology”, *Mikroniek*, vol. 50(2), p. 14–20.
- [3] Koster, M.P. (1998), “Constructieprincipes voor het nauwkeurig bewegen en positioneren”, 2nd ed., Twente University Press, ISBN 90-365-1135-6 (in Dutch).
- [4] Preumont, A. (2002), “Vibration control of active structures: An introduction”, 2nd ed., Kluwer Academic Publishers, ISBN 1-4020-0496-6.
- [5] Elliott, S.J. (2001), “Signal processing for active control”, Academic Press, ISBN 0-12-237085-6.

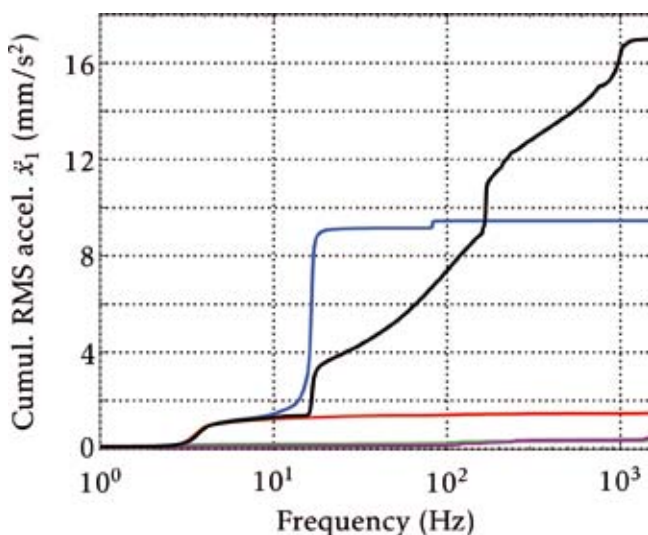


Figure 9. Cumulative spectrum of machine acceleration (mm/s²). (black: floor vibration; blue: passive; red: feedback; green: FF FIR; purple: FF IIR)

Acknowledgement

The research described in this article has been supported by the Innovation-oriented Research Programme (IOP) Precision Technology.

www.agentschapnl.nl/iopprecisietechnologie